

# Visual Early-Warning Signal Detection for Critical Transitions



Min Hu<sup>1, 3</sup>, Peng Jiang<sup>2, 3</sup>, Sheng-Chen Zhou<sup>1</sup>, and Yu-Feng Sun<sup>1</sup>

<sup>1</sup> SHU-UTS SILC Business School, Shanghai University Shanghai 201800, China  
20 Chengzhong Road, Shanghai, China  
{Minahu, jiangpengzq1991}@163.com

<sup>2</sup> Department of civil engineering, Shanghai University, Shanghai 200072, China  
49 Yanchang Road, Shanghai, China  
8860578@163.com

<sup>3</sup> Research Centre of Building industrialization, Shanghai University, Shanghai 200072, China  
49 Yanchang Road, Shanghai, China  
derek\_sun@yeah.net

Received 29 October 2015; Revised 09 February 2016; Accepted 18 April 2016

**Abstract.** Critical transitions occur in a wide variety of real systems, and it is very desirable to find early warning signals that a particular system may be approaching an undesired transition. This paper proposes an innovative visual method for critical transition detection, called TDTD (Time-series Data Trajectory Diagram). TDTD is a graphic tool used to time series data analysis, which can visualize the behavior of a trajectory of dynamic system. In order to go beyond the visual impression, Entropy Change Rate per Area (ECRA) is introduced as a universal indicator to analyze TDTD quantitatively, regardless difference in the details of each dynamic system. This method has been tested and compared with other related techniques in some fields, such as climate change and engineering disaster. The results of experiments indicate that TDTD is a valuable approach and reveals a new perspective for early detection of critical transitions.

**Keywords:** early warnings, time series, visualization technology

## 1 Introduction

Critical transitions, which occur when a complex system shifts abruptly from one state to another at a critical threshold or tipping point, play roles in a wide variety of systems. Examples include asthma attacks, epileptic seizures, financial market crashes, climate change, engineering disasters, and so on [1-3]. However, for these real natural or social systems, it is sometimes difficult to develop accurate models to predict thresholds of critical transitions or understanding all relevant mechanisms and feedbacks that influence the system. Thus, identification of early-warning signals may be a significant step forward when it comes to judging whether the probability of a critical transition increases.

Recently, in ecological systems [4-7], climate systems [8-9] and physiological systems [10], many studies have suggested that the proximity of a system to a tipping point can be detected by early warning signals. Many of these signals are mainly based on critical slowing down [7], a dynamical phenomenon occurring in the proximity of a bifurcation point where the timescale of recovery from perturbation tends to infinity. Increased autocorrelation, variance [7, 11], skewness [12], Employing Detrended Fluctuation Analysis (DFA) [13], spectral reddening [14], are all seen as early-warning signals.

Except common early-warning signals, many researchers tried to use visualization technology to reveal the characteristic structure of critical transitions in dynamic systems and detected meaningful hidden patterns in the time series data. Marchette and Solka extended the idea of color histograms to the data image package and used it for outlier detection [15]. Pinus view presents each item of the resulting hier-

archy and is utilized to identify the regime changes of the earth’s climate system [16]. Fu et al. extended VizTree by converting the time series to symbol string based on data point importance and this method was in abnormal change of stock data analysis [17]. Recurrence Plot (RP) [18], plot showing for trajectory of a dynamical dynamic system in phase space, has been used for the automated identification of abnormal electroencephalogram (EEG) signals. Although RP hasn’t been broadly used, it can detect outlier or regime shift without complete time series data.

In addition, results of some empirical studies have suggested that the dynamics of systems near a critical point have generic early-warning signals, which are built on common mathematical properties of phenomena. Nawrocki pointed out that bifurcation theory and entropy theory provide an appropriate analogue for the study of dynamic market disequilibrium [19]. Later, Kuehn used bifurcations, fast-slow systems and stochastic dynamics mathematical theories to classify critical transitions and detect tipping points [20]. Increasing studies are keen on exploring inherent factors in dynamic system through common mathematical properties of phenomena and bifurcation theory.

Despite these studies, identifying early-warning signals remains a challenge for real-life systems. First, many studies are based on simulated time-series data which are generated from a dynamic model, but the nature of simulated data has substantial differences with real-world data. For instance, in many cases, the common early-warning indicators are hard to be computed because the real-world data are high-dimensional and time complexity is high. Second, there is the absence of high frequency sampling data of dynamic systems and relevant information for inferring leading indicators. Third, there is no clear universal method for application of specific techniques or analyses in different fields, so different frameworks have been applied in different types of transitions.

This paper proposes a new visual method, the “Time-Series Data Trajectory Diagram” (TDTD), by which, time series data are plotted to express detailed dynamical processes and contribute to the identification of early-warning signals for abrupt changes in various systems. Each Time-Series Data Trajectory Diagram can reflect certain data subset, and decompose real overall time series data to two-dimensional diagrams, which makes the internal features of dynamic systems easier to show.

This paper is organized as follows: In section 2, a new two-dimensional coordinate system of concentric semi-circular coordinates is presented, followed by the introduction of the TDTD, which can express the features of a dynamic system. In section 3, combining potential leading indicators suggested in other theses with the dynamical features from TDTD, “Entropy Change Rate per Area” (ECRA) is defined and used as an early-warning indicator to detect critical transitions. In section 4, in order to demonstrate that the early-warning signal from TDTD can detect upcoming transitions in real systems and evaluate its performance, three cases in climate and underground engineering were analyzed and compared with other methods. In addition, we use bootstrap to verify likelihood of appearances of peaks in ECRA by randomness. Finally, in section 5, we summarize and draw some perspectives for future developments.

## 2 Time-Series Data Trajectory Diagrams

### 2.1 Basic Definition

We propose a new visual method TDTD to represent the characteristics of a dynamic system. Before we plot the TDTD step by step, some terms are essential to be declared, which are useful in discussing changes of dynamic systems and drawing process of TDTDs over time.

**Definition 1: Coordinate axes (Concentric semi-circular coordinates).** A Cartesian coordinate system specifies each point in a plane uniquely by a pair of numerical coordinates. It can only describe two-dimensional data and cannot meet the requirement to represent a multivariate state visually. Parallel coordinates [21], star coordinates [22] and concentric circle coordinates [23] are common ways of visualizing high-dimensional geometry and analyzing multivariate data. For avoiding different data that are mapped to the same point and limiting the data into a fixed range, we proposed a new coordinate system using concentric semi-circle axes to measure the degree of variation among states, in which the coordinate axes are organized as concentric semi-circles and broken lines represents the state.

On a plane with XY-Cartesian coordinates, we have drawn equidistant semi-circles that share the same center. They are  $n$  axes of the concentric semi-circle coordinates for  $n$ -dimensional Euclidean space  $R^N$ . Although these axes have different length, the axes have same range of angles ( $0-\pi$ ). Each semi-circle represents one axis, and whose direction is counter-clockwise. The  $P_i$  on  $d_i$ -axis represents the  $i^{th}$  dimen-

sional data component. Data points are scaled to the angle of the axis (with the minimum mapping to the right end of the axis and the maximum to the left end (see Fig. 1). In this way, we turn  $n$  dimensions into 2 dimensions, and it's easy to observe and find the abnormal place.

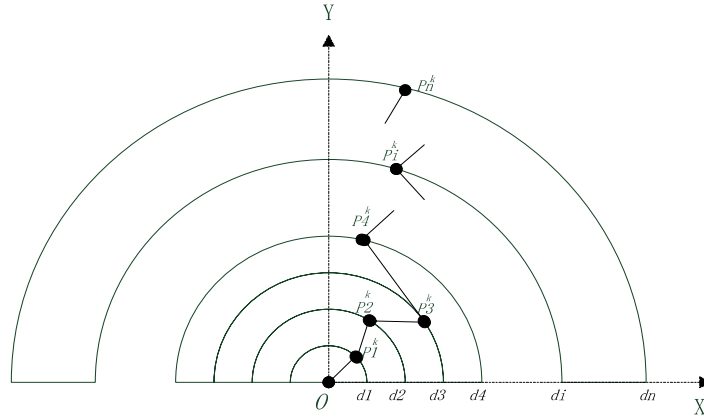


**Fig. 1.** Concentric semi-circular coordinates

**Definition 2: State.** At  $k^{th}$  moment, a set of time-series data generated by a dynamic system is depicted as  $S^k$ , and  $S^k$  is defined as the state of dynamic system at  $k^{th}$  moment in this paper.  $S^k$  is consist of  $n$ -dimensions, and  $P_i^k$  represents the  $i^{th}$  dimensional data component (see Fig. 1).

Furthermore,  $S$  is the overall process of dynamic system, and  $S^0$  is the state at initial moment:

$$S = \{S^0, S^1, \dots, S^{k-1}, S^k, S^{k+1}, \dots\} \tag{1}$$

**Definition 3: State Line.** If the state of system has  $n$  components ( $n$  dimensions) at  $k^{th}$  moment,  $P_i^k$  is defined as the  $i^{th}$  component ( $i^{th}$  dimension) of State  $S^k$  at  $k^{th}$  moment:

$$S^k = \{P_1^k, P_2^k, \dots, P_i^k, P_n^k\} \tag{2}$$

Where,  $P_i^k \in [min_i, max_i]$ ,  $min_i = \min\{P_i^k, 0 \leq k \leq S\}$ ,  $max_i = \max\{P_i^k, 0 \leq k \leq S\}$ .

And, it can be mapped to a point by using formula (3) and (4).

$$\theta_i^k = \frac{S_i^k}{max_i - min_i} \tag{3}$$

$$\begin{cases} P_i^k x = i * u * \cos(\theta_i^k) \\ P_i^k y = i * u * \sin(\theta_i^k) \end{cases} \tag{4}$$

Where,  $i * u$  is the different radii between two adjacent axis, and formula (3) can map  $P_i^k$  into  $0-\pi$  (see Fig. 1).

Thus, each state of a dynamic system can be represented as one unique broken line (see Fig. 2), called one state line. For state, it is represented by a broken line  $L^k$ , which consists of the connection of in sequence,  $1 \leq i \leq n$ .

$$L^k = \{0, P_1^k, P_2^k, \dots, P_i^k, P_n^k\} \tag{5}$$

The broken line is called state line, and each of these state lines represents the  $i^{th}$  dimension of state at  $n$  moment.

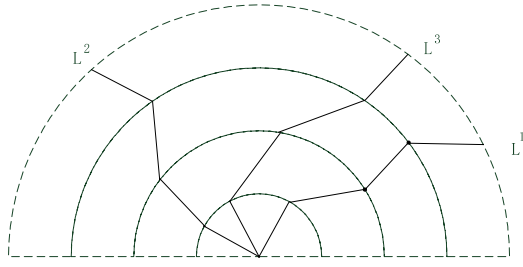


**Fig. 2.** State lines

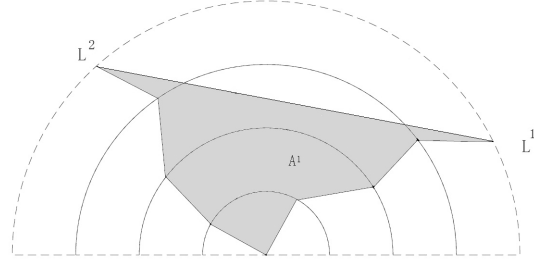


**Fig. 3.** State transition

**Definition 4: State Transition.** When a system evolves from state  $S^k$  to state  $S^{k+1}$ , a state transition occurs. If state  $S^k$  describes the feature of a dynamic system at  $k^{th}$  moment, state transition refers to the change from one state to another (see Fig. 3: state  $S^1$  to state  $S^2$  corresponds to state line  $L^1$  to state line  $L^2$ , and area  $A^1$  is state transition area). They are “close together” when the change between two states is small; otherwise they are “far apart”.

**Definition 5: State Trajectory.** As a dynamic system evolves, it undergoes a sequence of states in time order, which constitutes the state trajectory. For instance,  $\{S^i, S^{i+1}, \dots, S^{j-1}, S^j\}$  is called the state trajectory from  $i^{th}$  moment to  $j^{th}$  moment. In another word, one state trajectory is part of  $S$  (the overall process of dynamic system) (see Fig. 4).

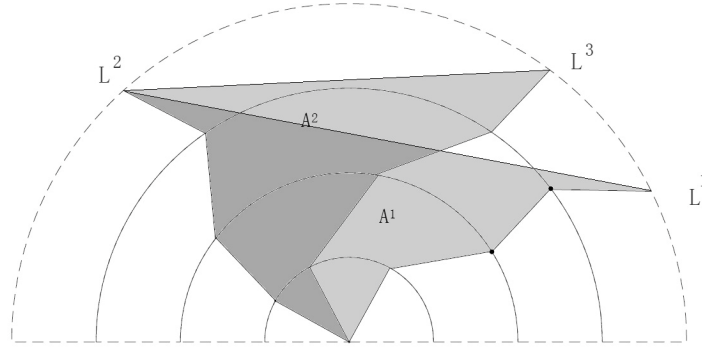


**Fig. 4.** Time series dynamic trajectory diagram

## 2.2 The Process of Plotting Time-Series Dynamic Trajectory Diagram

Time-Series Dynamic Trajectory Diagram (TDTD) can be used to describe the state trajectory (process of state transitions over a period of time). For example, from moment 1 to 3, the set of state trajectory is  $\{S^1, S^2, S^3\}$ , and the corresponding state lines' set is  $\{L^1, L^2, L^3\}$ . Cycle time  $T$  (span of time-window) of the state trajectory is 3.

The drawing process of TDTD is as follows:

**Step 1.** Drawing state lines  $\{L^1, L^2, L^3\}$  on the same graph with concentric semi-circle coordinates (see Fig. 2).

**Step 2.** For any two state lines that are close to each other, we plot a line between their endpoints to compose an enclosed region, and then fill color in this region. For instance,  $A^k$  is an enclosed region surrounded by State Line  $L^k, L^{k+1}$  and the connection line  $L^k L^{k+1}$  between their endpoints.

**Step 3.** Filling color in region  $A^1, A^2 \dots$  and  $A^{k-1}$  in time order, the color of overlapping parts is deeper when these regions are overlapped mutually, and the final color depth depends on the overlapping times (see Fig. 4).

**Step 4.** A sequence of the TDTDs for time series data is drawn according to cycle time  $T$  (span of time-window) and step  $D$  ( $0 \leq D \leq T$ ). That is to say, the data of first diagram sources from  $\{X_1, X_2, \dots, X_T\}$ , second diagram sources from  $\{X_D, X_{D+1}, \dots, X_{T+D}\}$ , and  $N^{th}$  diagram sources from

$\{X_{D*(N-1)}, X_{D*(N-1)+1}, \dots, X_{T+(N-1)}\}$ . Hence, different diagrams represent different state trajectory of dynamic system, which can reflect dynamic properties in different periods.

### 3 Quantification Assessment of TDTD

In order to detect critical transition in advance, we put forward a quantification assessment of TDTD. According to the shape and texture of diagram that is associated with the moment of critical transition in experiments and TDTD can reflect the fluctuation range of dynamic systems, we advance a graphical characteristic: image Entropy Change Rate per Area (ECRA), as the leading indicator to predict the critical transitions. To illustrate the meaning of ECRA, we introduce image entropy (E) and image area (A) first.

#### 3.1 Image Entropy

Image entropy is used to estimate the change in quantity of information among different pictures, which embodies the variation of dynamic systems among different periods of time. Based on the classic phenomenon of critical slowing down [7], increasing autocorrelation before the critical transition can be used as an early warning signal. And increasing autocorrelation means that the adjacent two states of the system become more and more similar. In other words, the same information of two adjacent states of the system increases, so the amount of information within a trajectory becomes small. The close connection between autocorrelation and entropy is the reason why we choose image entropy as a part of leading indicators. According to Shannon's entropy [6] in evaluating the information content of an image, the image entropy (E) of TDTD is defined by equation (6), (7).

$$E = -\sum_{i=0}^G d(i) * \log_2 d(i) \quad (6)$$

$$d(i) = \frac{p(i)}{N} \quad (7)$$

Where,

$G$ : the number of grey scale level of the images histogram,  $G$  is set at 0-255 in this paper.

$p(i)$ : the number of pixels whose gray scale level is  $i$ .

$N$ : the total number of pixels in the image.

$d(i)$ : the normalized frequency of occurrence when grey scale level is  $i$ .

#### 3.2 Image Area

Because of plotting mode of TDTD, the image area of TDTD can represent the fluctuation of dynamic systems. Image Area (A), is defined by equation (8), (9), represents the number of colored pixels in an image.

$$A = -\sum_{i=1}^X \sum_{j=1}^Y F(P_v(i, j)) \quad (8)$$

$$\begin{cases} F(a) = 1 & (a \neq 255) \\ F(a) = 0 & (a = 255) \end{cases} \quad (9)$$

Where,

$X$ : the pixel number in the horizontal direction of an image.

$Y$ : the pixel number in the vertical direction of an image.

$a$ : gray scale value from 0(black) to 255(white).

$P_v(i, j)$ : the gray scale value of a pixel at coordinates (i, j).

$F()$ : a function is used to judge whether the color of a pixel color is white or not.

### 3.3 Entropy Change Rate Per Area (ECRA)

Unlike Image Area and Image Entropy, which reflect the features of one diagram, Entropy Change Rate per Area (TDTD-ECRA) emphasizes on the change between the two adjacent diagrams. For two adjacent states trajectory diagrams, if their image entropy and area are  $H_i$ ,  $A_i$ , and  $H_{i-1}$ ,  $A_{i-1}$  respectively, ECRA () is defined by equation (10).

$$ECRA_i = \Delta HA_{i-1} = \frac{\frac{|H_i - H_{i-1}|}{H_i}}{A_{i-1}} = \frac{|H_i - H_{i-1}|}{H_{i-1} * A_{i-1}} \quad (10)$$

Where,

$\Delta HA_i$ : The entropy change rate per area of the  $i^{th}$  diagram.

$\Delta H_{i-1}$ : The entropy change rate of the  $i^{th}$  diagram.

$A_i$ : The area of the  $i^{th}$  diagram.

ECRA can identify the critical transition because it can reflect the change between two adjacent state trajectories and be more sensitive to abrupt shift of time-series data.

## 4 Experiments and Evaluation

In this section, TDTD is used for the experiments of climate change and underground engineering disaster, to verify the effectiveness of the method for visual early-warning detection. In addition, the leading indicator-ECRA is tested and compared with other common techniques.

### 4.1 Data Information

The first real date (Climate-1) is used to find a significant shift in climate history known as the “greenhouse–icehouse” transition. The second real date (Climate-2) is another well-known example of sharp changes in climate, which happened at the end of Younger Dryas and in which the average temperature suddenly jumped about  $10^\circ$  to a warmer state. The third real date (Engineering-1), which includes the risk signals in Shanghai Yangtze River Tunneling Project, is from underground engineering field. The data information, critical transition time and experiment parameters are listed in Table 1.

**Table 1.** Basic records info of three experiments

| Experiment  | Variable           | Number of records | Sample interval | Time range                | Time of Transition | T   | D  | Data Reference |
|-------------|--------------------|-------------------|-----------------|---------------------------|--------------------|-----|----|----------------|
| Climate-1   | CaCO3 (%)          | 968               | $10^4$ yrs      | $(39-32)*10^6$ years BP   | $34*10^6$ years BP | 100 | 5  | [24]           |
| Climate-2   | Cariaco Grey scale | 2770              | 0.5yr           | $(1.25-1.12)*10^4$ yrs BP | 11,570yrs BP       | 200 | 5  | [25] [26]      |
| Engineering | Cabin Pressure1~5  | 10563             | 3 min           | 2008/5/1–2008/5/22        | 2008/5/19 14:00    | 240 | 15 | [27]           |

### 4.2 Experiment Results and Analysis of TDTD

We plot TDTDs of different data by different cycle time T and step D. And three groups of TDTDs are numbered in time order.

Fig. 6(a)-(c) show some TDTDs of three real data, the two adjacent diagrams are similar at most of time, but we find some obvious changes in the Diagram No. 128 of Climate-1 experiment, No. 343 of Climate-2 experiment, and No. 1491 of Engineering-1. The time of these diagrams is 34.32 million years BP, 11,624 years BP and 2008/5/17 0:03 respectively, which are close but lead to the actual critical transition time. Due to large data set, the diagrams only in vicinity of the critical transition are showed. In Fig. 6 (a), we can directly see the area and the structure of No.122-127 diagrams are almost the same, and No.128 changed a lot compared with No.122-127. So, we regard it as an alarm. Similarly, the diagrams of

two other experiments highlighted in Fig. 6 (b)-(c), have suddenly changed and they are not the same as diagrams before. Through these highlighted diagrams we could detect that the changes happened in different dynamic systems easily.



**Fig. 6. (a)** Partial TDTDs of Climate-1 experiment



**Fig. 6. (b)** Partial TDTDs of Climate-2 experiment



**Fig. 6. (c)** Partial TDTDs of engineering experiment

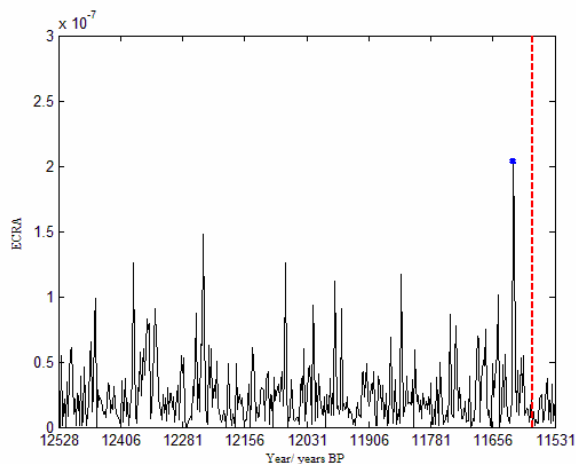
#### 4.3 Experiment Results and Analysis of ECRA

Fig. 7 (a)-(c) respectively shows the change curve of ECRA indicator, which is quantification assessment of TDTD over time, and the vertical dashed line stands for the real sudden shift that happened with time. There exist notable peaks, which are identified as early-warning signals, tagged with a blue point before critical transition.

For Climate-1 experiment, the warning signal of ECRA is not only in advance, but also easy to be caught. The warning signal of ECRA alarms 4 million years in advance and warning peak is nearly 5 times as high as average of first half ECRA curve.

For Climate-2 experiment, ECRA indicators hit local highs at 11618 years BP, the scale of a peak to 4 times of the average of first half ECRA curve.

There are two peaks of TDTD-ECRA in Fig. 7 (c), two time points of 5/1713:44 and of 5/198:29 are before real risk happened. The two peak points of ECRA are about 11 times and 14 times as high as average top 50% of ECRA curve respectively. Therefore, two early-warning signals are strong enough to be distinguished, and first signal is 2 days earlier than the incident occurred. In this experiment, the ECRA indicator is useful because of the advantage of enough lead-time, to allow prevention of hazards.



**Fig. 7. (a)** ECRA curve of Climate-1 experiment

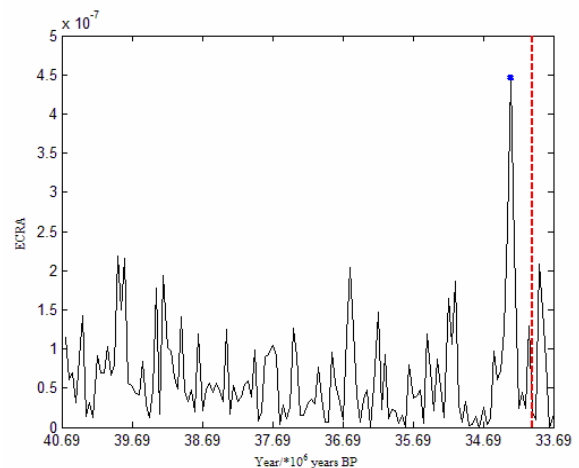


**Fig. 7. (b)** ECRA curve of Climate-2 experiment

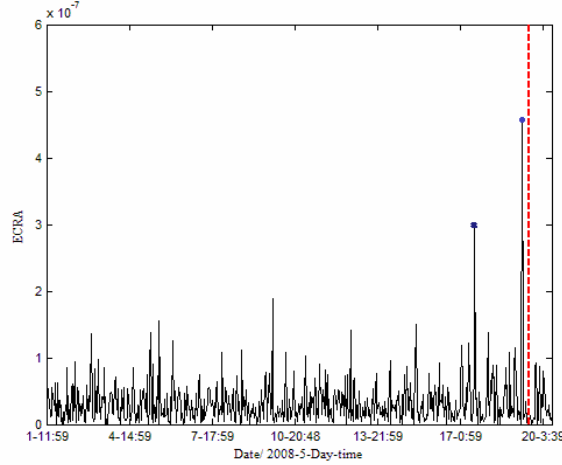


Fig. 7. (c) ECRA curve of engineering experiment

#### 4.4 Statistical Analysis

Though experiments above, we verify that the peaks, which are several times of average ECRA curves, can work as early warning signals. In order to make sure that the peaks only appear before regime shifts, in other words, the occurrence of these peaks is not due to random disturbance. We test the likelihood of obtaining peaks in ECRA by random; we created surrogate time series by bootstrap method.

**Bootstrap.** Before beginning the main analysis of surrogate time series, we will describe how bootstrap works [28]. Suppose that our data consist of a random sample from unknown probability distribution  $F$  on the real line,

$$X_1, X_2, \dots, X_n \sim F \quad (11)$$

Having observed  $X_1 = x_1, X_2 = x_2, \dots, X_n = x_n$ , we compute the sample mean  $\bar{x} = \sum_{i=1}^n \frac{x_i}{n}$ , and wonder how accurate it is as an estimate of the true mean  $\theta = E_F\{X\}$ .

If the second central moment of  $F$ :

$$\bar{\sigma}(F) = \left[ \frac{\mu_2(F)}{n} \right]^{\frac{1}{2}} \quad (12)$$

The shortened notation  $\sigma(F) = \sigma(F; n, x)$  is allowable because the sample size  $n$  and statistic of interest  $\bar{x}$  are known, only  $F$  being unknown. The standard error is the traditional measure of  $\bar{x}$ 's accuracy. Unfortunately, we cannot actually use (12) to access the accuracy of  $\bar{x}$ , since we do not know  $\mu_2(F)$ , but we can use the estimated standard error,

$$\bar{\sigma} = \left[ \frac{\bar{\mu}_2}{n} \right]^{\frac{1}{2}} \quad (13)$$

Where  $\bar{\mu}_2 = \sum_{i=1}^n (x_i - \bar{x})^2 * (n-1)$ , the unbiased estimate  $\bar{\mu}_2(F)$ .

There is more obvious way to estimate  $\sigma(F)$ . Let  $\hat{F}$  indicate the empirical probability distribution.  $\hat{F}$ : Probability mass  $1/n$  on  $x_1, x_2, \dots, x_n$

Then we can simply replace  $F$  by  $\hat{F}$ , obtaining

$$\bar{\sigma} \equiv \bar{\sigma}(\hat{F}) = \left[ \frac{\mu_2(\hat{F})}{n} \right]^{\frac{1}{2}} \quad (14)$$

as the estimated standard error for  $\bar{x}$ . This is the bootstrap estimate.

**Analysis of the surrogate time series.** Because the early warning is based on some high peaks in the ECRA which contains many peaks of varying height, we test against a null model of what an equivalent system that isn't approaching a critical transition would produce in terms of an ECRA plot - no doubt it would have peaks - so we use a statistical criterion for saying that the peaks seen in the experiments (see Fig. 6) are outside the distribution from the null model with some level of confidence (P-value). We bootstrapped our datasets by reshuffling the order of the original time series and by picking data with replacement to generate surrogate records of similar probability distribution (mean and variance), and we use 1000 surrogate time series data to get 1000 TDTDs and ECRA. Then, we estimated the probability that the peaks as early warning signals would be observed by chance as the fraction of the 1,000 ECRA curves which haven't critical transitions.

The probability estimates for data peaks as early warning signals before the critical transition under the  $H_0$  hypotheses are shown in Table 2. Very low probabilities were estimated in the records of the transitions of the Climate-1, the Climate-2 and Engineering experiment. Its proof that the peaks, which are several times of average ECRA curves, are only affected by regime shifts rather than the randomness of dynamic systems. That means the peaks, which are seen as early warning signals, won't appear in non-critical-transition dynamical systems.

**Table 2.** Probability of acquiring the estimated values for the peak statistic of the original time series under  $H_0$  hypotheses for a set of 1,000 surrogate time series

| Experiment    | $H_0$   |
|---------------|---------|
| Original data | Peaks   |
| Climate-1     | 0.004** |
| Climate-2     | 0.005** |
| Engineering   | 0.014** |

*Note.* Under  $H_0$ , data sets are created by bootstrapping.

\*  $p < 0.1$ . \*\*  $p < 0.05$ .

#### 4.5 Performance Comparison

To further verify the performance of ECRA, we select two typical methods for detecting critical transition complex systems to do comparative experiments. One is early warning signals, the other is recurrence plot (including recurrence quantification analysis). In our experiments, the software packages of two methods are from <http://www.early-warning-signals.org/> and <http://tocsy.pik-potsdam.de/CRPtoolbox/>.

**Early Warning Signals.** Increasing autocorrelation at-lag-1 (AR (1)) and increasing variance as standard deviation (SD) are main metrics-based indicators prior to the transition<sup>1</sup>.

We computed two metrics within rolling windows (window size = 10% of time series length, bandwidth = 5% of time series length) for Climate-1 original time series (see Fig. 8(a)), AR1 increase up to the transition with a strong trend, while SD decreased ( $\tau = -0.081$ ). Similarly, the experiment results of Climate-2 (window size = 50%, bandwidth = 5%) and engineering (window size = 40%, bandwidth = 5%) time series were shown in Fig. 8(b) and Fig. 8(c) as well. AR1 generally increased ( $\tau = 0.082$  and  $\tau = 0.669$ ). And SD decreased in Climate2- Experiment, while SD increased almost linearly up in Engineering Experiment. It's obvious that the performance of AR1 and SD as early warning signals for critical transitions is not unstable and reliable. Although AR1 shows a good effect, the early warning signals do not have accurate time points. They can hardly provide sufficient warning time in advance to adapt management to avoid a regime shift.

**Recurrence Plots.** Recurrence Plots (RPs) and related methods are widely accepted graphic tools for data analysis in various disciplines. Some recurrence quantification analysis (RQA) measures, such as laminarity (LAM) and determinism (DET), become significant measures for dynamical transition analysis [29]. The time dependent RQA analysis is based on moving windows, shifting the time series and calculating the RPs within these windows.

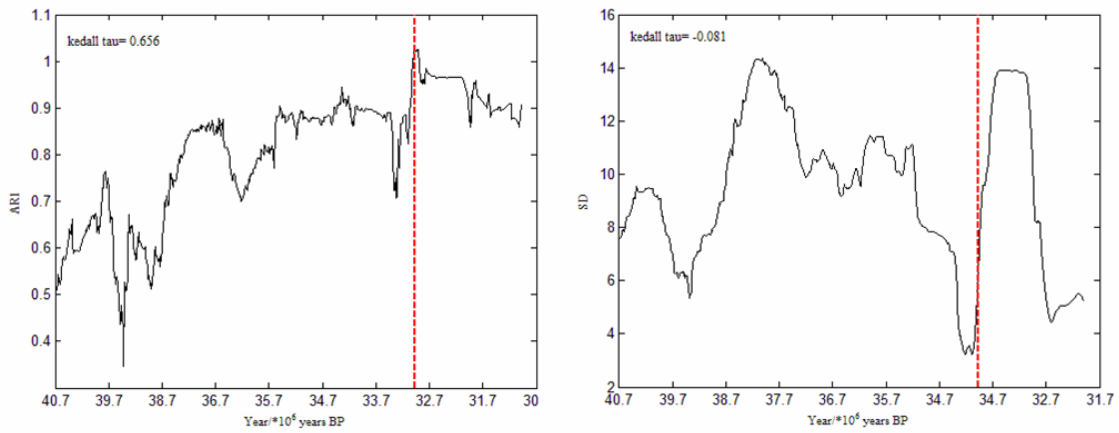


Fig. 8 (a) Early-warning signals of Climate-1 experiment

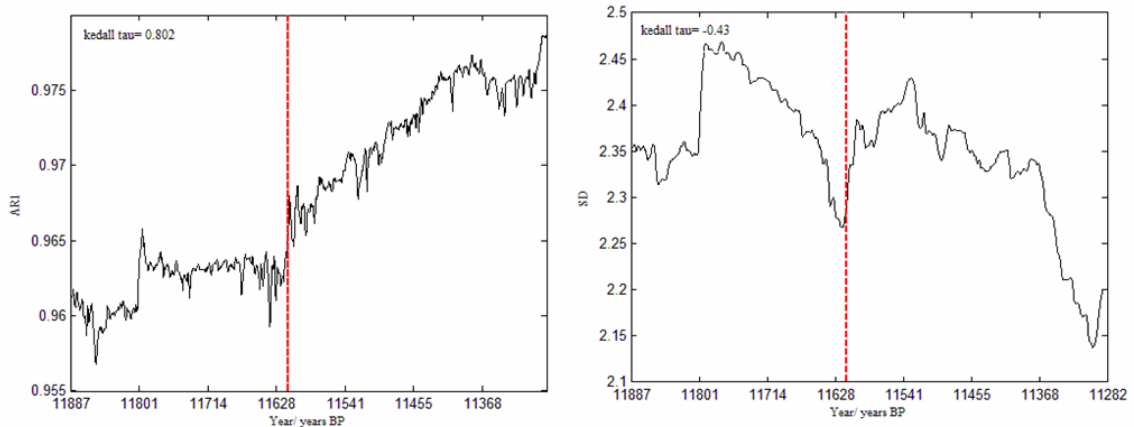


Fig. 8. (b) Early-warning signals of Climate-2 experiment

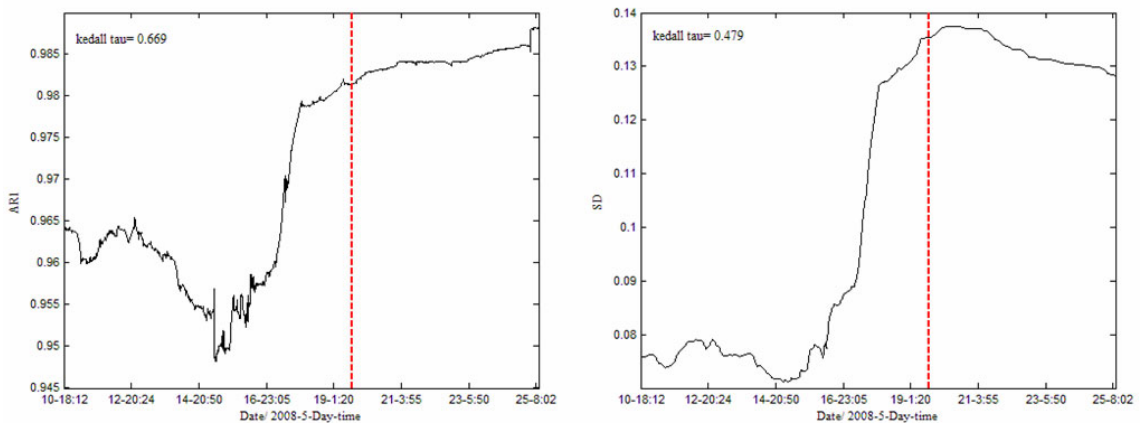


Fig. 8. (c) Early-warning signals of engineering experiment

The experiment of Climate-1 includes recurrence plot, DET and LAM indicator curves, in which the embedded dimension is 4 and delay is 6. The early warning time is  $34.06 \times 10^6$  years BP. We found no obvious warning signal of transition in DET and LAT curves. The experiment results with the embedded dimension of 4 and delay of 9 based on Climate-2, and the warning time is 11,097 years BP, which lagged to the actual transition time. Similarly, the transition point of engineering experiment at 2008/5/16 11:56 is prior to the actual transition with embedded dimension of 5 and delay of 10.

It is thus clear that RPs often lags behind the time of actual transition and the performance of DET and LAM is uncertain, although they can detect the critical transition clearly.

**Conclusion of performance comparison.** Table 3 summarize the experiment results of ECRA, early warning signals (AR1 and SD) and RP. For three different experiment data, only ECRA forecast the critical transition prior to the actual transition. Early warning signals (AR1 and SD) can hardly give an actual alarm time point to avoid a regime shift. Meanwhile, RPs is not always valid and robust, due to limitation by the parameters of embedded dimension and delay time. In addition, RP is also not a timely identification and forecasting method for critical transition because it depends on the data statistical analysis. In comparison, ECRA is better than the existing typical visual methods and metric-based indicators for detecting critical transition in advance, with the advantages of low computational complexity, high sensitivity and robustness.

**Table 3.** Comparison of three methods for transition warning performance

| Experiment  | Time of Critical transition | Time of Warning Critical Transition |   |                                | The most effective method |
|-------------|-----------------------------|-------------------------------------|---|--------------------------------|---------------------------|
|             |                             | ECRA                                | Early Warning Signal                              | RP                             |                           |
| Climate-1   | 34*10 <sup>6</sup> years BP | 34.42*10 <sup>6</sup> years BP      | 33.7*10 <sup>6</sup> —34*10 <sup>6</sup> years BP | 34.06*10 <sup>6</sup> years BP | ECRA                      |
| Climate-2   | 11,570 years BP             | 11,638 years BP                     | 11630-11570years BP                               | 11,097 years BP                | ECRA                      |
| Engineering | 2008/5/19 14:00             | 2008/5/1713:44                      | 2008/5/15-2008/5/18                               | 2008/5/16 11:56                | RP                        |

## 5 Conclusion and Future Works

Early warning for critical transition is a complex and challenging problem. In this paper, we described an innovative visualization method for critical transition detection, called the Time-Series Data Trajectory Diagram (TDTD), to reveal trends and features before abrupt change of a dynamic system. Each diagram reflects certain data subset, so real overall time series data are decomposed to state trajectory diagrams, which make the internal features of dynamic systems easier to show. TDTD emphasizes the change process of data values, weakening the influence of time factors, so TDTD is very robust for missing and noisy data.

Experiments using TDTD to predict critical transitions in climate and underground engineering indicate that it is a valuable approach. Experiments demonstrate that adjacent TDTD often change dramatically before critical transition happen. As an indicator, ECRA is used to measure TDTD, which not only delivers a numerical measure, but also represents the potential information in time series of complex systems. And TDTD-ECRA is a universal indicator among the three kinds of indicators to identify an upcoming critical transition successfully.

In comparison to other methods, TDTD doesn't require specific data-treatment to yield sensible signals, while it can pre-warn critical transitions effectively and clearly. This is encouraging as it may reduce the chance of false alarms. Of course, the possibility of missed signals is difficult to be eliminated fully.

However, many problems are still worth researching in the future. First, in our experiments, we found that the accuracy and sensitivity of detecting critical transitions are related to the key parameters (cycle time  $T$  and step  $D$ ) of TDTDs. Therefore, research on setting rules for these parameters combined with the specific fields and issues is important. Second, there was only one experiment of multidimensional data evaluated in this paper. Testing TDTD in more real multidimensional datasets is the next step. The last but most importantly, TDTD is a useful visual method to represent features for time series data of dynamic systems. We recommend researchers in different fields to evaluate TDTD and innovate more interesting method with TDTD for time series data of dynamic systems in other fields, such as logical (e.g. patterns of gene expression), medical (e.g. predicting epileptic seizures), physiological (e.g. respiratory rhythms), or social (e.g. numbers of tweets) situations.

## Acknowledgment

The authors would like to thank the anonymous referees and the editor for their valuable opinions. This

work was supported by Shanghai Science and Technology Development Funds (13511504803, 12DZ0512500).

## References

- [1] M. Scheffer, J. Bascompte, W.A. Brock, V. Brovkin, S.R. Carpenter, V. Dakos, E.V.H. Nes, M. Rietkerk, G. Sugihara, Early-warning signals for critical transitions, *Nature* 461(7260)(2009) 53-59.
- [2] M. Scheffer, *Critical Transitions in Nature and Society*, Princeton University Press, Princeton, 2009.
- [3] J.M. Drake, B.D. Griffen, Early warning signals of extinction in deteriorating environments, *Nature* 467(7314)(2010) 456-459.
- [4] R.D. Batt, W.A. Brock, S.R. Carpenter, J.J. Cole, M.L. Pace, D.A. Seekell, Asymmetric response of early warning indicators of phytoplankton transition to and from cycles, *Theoretical Ecology* 6(3)(2013) 285-293.
- [5] S.R. Carpenter, W.A. Brock, J.J. Cole, M.L. Pace, A new approach for rapid detection of nearby thresholds in ecosystem time series, *Oikos* 123(3)(2014) 290-297.
- [6] S. Kéfi, V. Guttal, W.A. Brock, S.R. Carpenter, A.M. Ellison, V.N. Lavina, Early warning signals of ecological transitions: methods for spatial patterns, *Plos One* 9(3)(2014) 92-97.
- [7] V. Dakos, M. Scheffer, E.H. van Nes, V. Brovkin, V. Petoukhov, H. Held, Slowing down as an early warning signal for abrupt climate change, *PNAS* 105(38)(2009) 14308-14315.
- [8] H. Held, T. Kleinen, Detection of climate system bifurcations by degenerate fingerprinting, *Geophysical Research Letters*, 31(23)(2004) L23207.
- [9] H. Wu, W. Hou, P.C. Yan, Using the principle of critical slowing down to discuss the abrupt climate change, *Acta Physica Sinica* 62(3)(2013) 221-229.
- [10] R. Compton, H. Moon, LU. Tc, Catastrophe prediction via estimated network autocorrelation. <<http://www.freepatentsonline.com/9020875.html>>, 2011.
- [11] N. Medicine, Prediction of epileptic seizures: are nonlinear methods relevant? *Nature Medicine* 9(3)(2003) 241-242.
- [12] V. Guttal, C. Jayaprakash, Changing skewness: an early warning signal of regime shifts in ecosystems, *Ecology Letters* 11(5)(2008) 450-460.
- [13] V.N. Livina, T.M. Lenton, A modified method for detecting incipient bifurcations in a dynamical system, *Geophysical Research Letters* 34(3)(2007) 145-149.
- [14] T. Kleinen, H. Held, G. Petschel-Held, The potential role of spectral properties in detecting thresholds in the earth system: application to the thermohaline circulation, *Ocean Dynamics* 53(2)(2002) 53-63.
- [15] D.J. Marchette, J.L. Solka, Using data images for outlier detection, *Computational Statistics & Data Analysis* 43(4)(2003) 541-552.
- [16] M. Sips, P. Kothur, A. Unger, H.C. Hege, D.A. Dransch, A visual analytics approach to multiscale exploration of environmental time series, *IEEE Transactions on Visualization and Computer Graphics* 18(12)(2012) 2899-2907.
- [17] T.C. Fu, F.L. Chuang, K.Y. Kwok, C.M. Ng, Stock time series visualization based on data point importance, *Engineering Applications of Artificial Intelligence* 21(8)(2008) 1217-1232.
- [18] U.R. Acharya, S.V. Sree, S. Chattopadhyay, W. Yu, P.C. Ang, Application of recurrence quantification analysis for the automated identification of epileptic EEG signals, *International Journal of Neural Systems* 21(3)(2011) 199-211.
- [19] N. David, Entropy, bifurcation and dynamic market disequilibrium, *Financial Review* 19(2)(1984) 266-284.

- [20] C. Kuehn, A mathematical framework for critical transitions: bifurcations, fast-slow systems and stochastic dynamics, *Physical D-nonlinear Phenomena* 240(12)(2011) 1020-1035.
- [21] A. Inselberg, B. Dimsdale, Parallel coordinates: a tool for visualizing multi-dimensional geometry visualization, in: *Proc. the First IEEE Conference*, 1991.
- [22] E. Kandogan, Star coordinates: a multi-dimensional visualization technique with uniform treatment of dimensions, in: *Proc. the IEEE Information Visualization Symposium Late Breaking Hot Topics*, 2009.
- [23] J.W. Zhang, Y. Wen, Q.V. Nguyen, L.F. Fu, M.L. Huang, J.D. Yang, J.Z. Sun, Multi-dimensional data visualization by using concentric circle coordinates, in: Huang M., Nguyen Q., Zhang K. (Eds.), *Visual Information Communication*, Springer, Boston, MA, September 30, 2009, pp. 95-118.
- [24] A. Tripathi, J. Backman, H. Elderfield, P. Freretti, Eocene bipolar glaciation associated with global carbon cycle changes, *Nature* 436(7049)(2005) 341-346.
- [25] K.A. Hughen, J.R. South, S.J. Lehman, J.T. Overpack, Synchronous radiocarbon and climate shifts during the last deglaciation, *Science* 290(5798)(2000) 1951-1954.
- [26] S. Gulliksen, H.H. Birks, G. Possnert, J. Mangerud, A calendar age estimate of the Younger Dryas-Holocene boundary at Kråkenes, western Norway, *The Holocene* 8(3)(1998) 249-259.
- [27] M. Hu, F.F Wu, B. Zhu, B. Lu, J.L. Pu, A new hazard identification method-state transition graph, *Applied Mechanics and Materials* 48-49(1)(2011) 71-78.
- [28] B. EFRON, Bootstrap methods for standard errors, confidence intervals, and other measures of statistical accuracy, *Statistical Science* 1(1)(1986) 54-75.
- [29] N. Marwan, S. Schinkel, J. Kurths, Recurrence Plots 25 years later- gaining confidence in dynamical transitions, *Euro physics Letters* 101(2)(2013) 20007.

